frontiers in Physics

ORIGINAL RESEARCH
published: 25 October 2021
doi: 10.3389/fphy.2021.722173

# Wireless Textile Moisture Sensor for Wound Care

*Marta Tessarolo*[1*†], *Luca Possanzini*[1*†], *Isacco Gualandi*[2], *Federica Mariani*[2], *Leo Davide Torchia*[1], *Danilo Arcangeli*[2], *Federico Melandri*[3], *Erika Scavetta*[2] *and Beatrice Fraboni*[1]

[1]*Department of Physics and Astronomy "Augusto Righi", Alma Mater Studiorium Università di Bologna, Bologna, Italy,* [2]*Department of Industrial Chemistry "Toso Montanari", Alma Mater Studiorium Università di Bologna, Bologna, Italy,* [3]*Plastod s.p.a, Bologna, Italy*

One of the main problems of hard-to-heal wounds regards the monitoring of their healing progress. Currently, clinicians monitor the wound's status by removing the dressing, disturbing the healing process. A relevant parameter that they need to monitor is wound moisture. Indeed, a low amount of exudate can desiccate the wound, while a high level of moisture will lead to maceration. Thus, to optimize the healing process, it is particularly important to maintain an optimum level of moisture, while limiting unnecessary dressing changes. An innovative solution to address this issue is the design of a bandage with an integrated moisture sensor. In this work, we developed a textile sensor based on a conductive polymer poly(3,4-ethylenedioxythiophene):polystyrene sulfonate (PEDOT:PSS) that discriminates wound's moisture level. PEDOT:PSS is screen printed on a gauze in a specific geometry. Exploiting its intrinsic electrochemical properties, the sensor operates in real time by monitoring impedance variations that span over several orders of magnitude between dry and wet states. The sensor is directly integrated with an RFID chip, implementing a real-time wireless monitoring. The final device results in a low-cost, user friendly, disposable and wirelessly connected patch.

**Keywords: healing state, PEDOT:PSS, wound, smart bandage, moisture sensor**

OPEN ACCESS

***Edited by:***
*Marta Mas-Torrent, Consejo Superior de Investigaciones Científicas (CSIC), Spain*

***Reviewed by:***
*Javier Hernández Ferrer, Institute of Carbochemistry (CSIC), Spain*
*Giorgio Mattana, Université de Paris, France*

***Correspondence:**
*Marta Tessarolo*
*marta.tessarolo3@unibo.it*
*Luca Possanzini*
*luca.possanzini2@unibo.it*

*†These authors have contributed equally to this work and share first authorship*

***Specialty section:***
*This article was submitted to Interdisciplinary Physics, a section of the journal Frontiers in Physics*

***Received:*** *08 June 2021*
***Accepted:*** *29 September 2021*
***Published:*** *25 October 2021*

***Citation:***
*Tessarolo M, Possanzini L, Gualandi I, Mariani F, Torchia LD, Arcangeli D, Melandri F, Scavetta E and Fraboni B (2021) Wireless Textile Moisture Sensor for Wound Care. Front. Phys. 9:722173. doi: 10.3389/fphy.2021.722173*

## INTRODUCTION

Wound healing is an essential physiological process by which damaged tissues repair themselves. If normal progression is disrupted, the wound enters a pathologic inflammation state characterized by impaired healing, which can eventually lead to chronicity [1,2]. Chronic wounds significantly affect a patient's quality of life, imply high treatment costs and are correlated with high mortality in bedridden and diabetic patients [3,4].

The healing process of a wound depends on several factors such as moisture level, pH, temperature, uric acid, lactate and glucose levels as well as infection status [5]. Among them, the most relevant is the moisture: a low exudate level can desiccate the wound and slow down the recovery, while high moisture level could lead to wound maceration [6]. Optimal moisture level in the wound bed is crucial for proper tissue regeneration. In daily practices, wound assessment is mainly based on a visual inspection [7]. The clinicians perform a qualitative assestment of the wound's status by removing the dressing, with the consequence of disturbing the healing process. A quantitative analysis of exudate is obtained by measuring the weight of the dressing before and after use [8]. Therefore, the possibility to monitor the moisture level of a

wound in real-time, without removing the dressing, could significantly improve the quality of wound management, avoid unnecessary dressing changes and personalized therapies [9].

Nowadays, miniaturized wearable sensors and readers have been developed. Many body fluids such as sweat [10], tears [11] or saliva [12] are exploited to monitor relevant biomarkers for healthcare applications. However, the wound environment is still poorly investigated. One relevant reason is the biocompatibility required to be in contact with damaged skin. Moreover, the high complexity of wound exudate and wide range of wound morphologies limits the application of the most common sensors [5,13]. Recent examples of smart bandage have been proposed for the detection of pH [14–16], uric acid and Bacteria infection [17,18].

Concerning wound moisture, a possible strategy to implement a moisture sensing bandage is to integrate a relative humidity (RH) sensor and assume that, as RH increases towards 100%, it indicates that the dressing is becoming saturated with exudate and needs replacing [13,19,20]. In the field of wearables, humidity textile sensors have attracted significant attention due to the intrinsic hydrophilicity properties of fabric/fiber materials that help humidity sampling. As regards the sensing configuration and mechanism, different working principles have been reported: capacitive, resistive and impedance-based. An example of capacitive sensor is based on polyamide fibers covered with copper threads [21]. The polymer works as the dielectric material, while copper as the conductive electrode. A change in the RH reversibly alters the whole capacitance of the yarn sensor. In a different approach, carbon nanotubes (CNTs) were dispersed in a polymer matrix such as poly(vinyl alcohol) (PVA) [22] or polylactide (PLA) [23]. CNTs network is used to create a good electrically conductive path, while PVA or PLA are hygroscopic polymers which swells via water absorption modifying the conductive network and resistivity. Lastly, impedance-based RH sensors are commonly composed of two adjacent electrodes, typically interdigitated and covered with a humidity-sensitive film. For example, Li et at [24]. deposited Ni interdigitated electrodes onto silk and covered them with graphene oxide (GO) suspension to produce a RH sensor. As an alternative, humidity sensing layers based on poly(3,4-ethylenedioxythiophene):polystyrene sulfonate (PEDOT:PSS) have been proposed due to their hygroscopic behavior [25–27].

Although several examples of humidity sensors have been reported in the literature, most of them have been developed for breath monitoring, measuring RH in the air. These sensors have never been tested in a wound environment and an actual correlation with RH and bandage saturation has not been demonstrated yet. Instead of measuring RH, which is mainly related to humidity in air, it is better to focus on moisture sensors in order to quantify the actual volume of exudate soaking the bandage.

The first example of a smart bandage integrating a moisture sensor was presented by McColl et al. in 2007 [28]. The proposed sensor consists of two Ag/AgCl electrodes insulated with silicon and inserted in a commercial dressing. Exploiting the ionic nature of exudate, they measured the impedance variation across the two electrodes with an AC measurement. They obtained a correlation between the change in impedance and moisture loss, thus enabling a direct comparison among different fabric properties on retained moisture. Thanks to this first approach, various bandage fabrics have been developed with different absorption and retention properties in the last decade [5] and in 2016 a commercial moisture sensor for wound care was developed called "Wound Sense" [29]. The system is composed of a plastic-based sensor consisting of Ag/AgCl electrodes and connected to a bulky reader, which disturbs the regular movements of the patient. The moisture reading is visually shown as a five-drop scale (dry, moist to dry, moist, wet to moist, wet) but no quantitative correlation with the effective amount of exudate is given, and the reversibility is not guaranteed.

In this work, we propose a moisture impedance sensor based on PEDOT:PSS embedded into a commercial bandage for wound healing management. The performance of the moisture sensor was studied using different geometries to extract two parameters: 1) the threshold exudate volume to distinguish between a dry and wet wound and 2) saturation exudate volume. Several patch configurations based on materials with opposite hydrophilicity properties have been compared. The sensor operates in real-time and its impendence varies over several orders of magnitude between the dry and the wet states. The drastic change in the sensor impedance was exploited for interfacing the smart dressing with an RFID read-out technology, thus implementing wireless and fully passive monitoring. By combining different bandage layers, the final device can be adapted for several types of wound, or for different stages of healing process with different optimum moisture conditions.

## MATERIALS AND METHODS

### Chemicals

PEDOT:PSS, with the trade name of Clevios PH1000, was purchased from Heraeus. Ethylene glycol, sodium chloride, calcium chloride and iodine were purchased from Sigma Aldrich. All the chemicals were used as received. The conductive ink was prepared by mixing and sonicating PEDOT:PSS and ethylene glycol in the ratio 0.95:0.05. The viscous ink, needed for the screen printing procedure, was obtained by evaporating the 60% of the initial weight warming the solution at 70°C in an oven as previously reported [30] . The simulated thin wound exudate was prepared according to a standard recipe (Solution A) [28] by mixing 0.142 M NaCl, and 0.0025 M $CaCl_2$ in distilled water. The as-prepared artificial solution presents a viscosity equivalent to water.

### Substrate

The textile wound dressing materials used to fabricate the moisture sensor can be divided into three types: the protective layer that is in contact with the skin, the active layer containing the conductive and sensitive pattern, and the reservoir textile that stores the absorbed exudate. Two textile-based substrates differing from thickness and material composition were investigated as supports for the active layer. The first gauze,

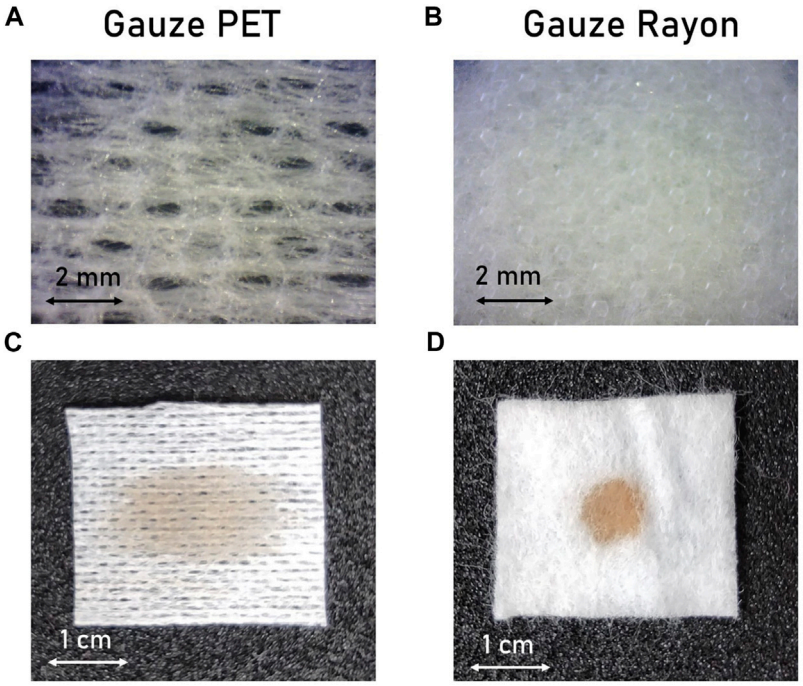


**FIGURE 1 |** Active gauze textile substrates. **(A–B)** Enlarged top view and **(C–D)** top view photos of the active substrates showing the different spreading of a colored liquid through the textile surface of PET and Rayon gauzes.

called "Gauze Rayon," is made of 70% rayon, 30% polyethylene terephthalate and a thin anti-adherent film of polyethylene. The second gauze, called "Gauze PET," is composed by 100% polyethylene terephthalate. Two different textile-based reservoirs were used as the third layer to study the impact of a different absorption behavior on the sensor's response. Their scope is to continuously drive the sampled wound exudate across the sensing layer. The first one, called "Abs layer PE," is composed by two layers, one of polyethylene and the other of rayon, while the second one, called "Abs layer C," is formed by a polyurethane foam and a cellulose-based textile.

## Sensors Fabrication

The moisture sensor fabrication is a two-step procedure that firstly consists of the active material deposition, and secondly in the assembly together of three different textile-based layers to obtain a smart and sensitive wound dressing. The deposition procedure was carried out with a serigraphy frame in which two straight non-consecutive PEDOT:PSS-based strips (an amount of (93 ± 7) mg) were coated onto the gauzes. After the deposition, the ink was dried at 70°C for 30 min. Two consecutive steps led to a homogeneous and highly conductive layer. Moreover, the geometry can be easily changed by modifying the mask pattern according to the desired performance. The electrical contacts were formed by two stainless-steel conductive threads sewn onto the conductive coating. The final smart wound dressing was realized by heat-sealing together in a stacked structure three textile layers: the protective, active and reservoir ones.

## Characterization

Fluid absorption at the wound dressing plays a key role in chronic wounds treatment. Here, the absorption ability of the textile substrates was measured following the international procedure UNI EN ISO 9073-6; 2004. Briefly, the weight of a 25 × 25 mm gauze was measured before (mi) and after ($m_f$) immersion in artificial exudate and the liquid absorption was calculated as $(m_f\text{-}m_i)/m_i$ *100.

The moisture sensor characterization was performed by monitoring the change in the device impedance after increasing additions of artificial exudate (**Supplementary Figure S1** 1). An AC signal with a peak voltage of 100 mV was applied and the resulting current measured by the MFLI Lock-in Amplifier by Zurich Instruments. The working frequency used in all the reported cases was 1 KHz and it was chosen after an impedance spectroscopy investigation.

The main parameters used to characterize the moisture sensors behavior are the threshold volume, which is the amount of liquid needed to drop the device impedance under a target value of 50 kΩ, and the saturation volume, which represents the maximum quantity of exudate that can induce a detectable and significant impedance variation. These values are extracted by plotting in log-log scale the impedance versus volume data. Two linear regimes compose the typical trend of these plots and allow us to calculate the threshold and saturation volume. The first one is computed by the intersection of the linear fitting curve with 50 kΩ, while the second one is extracted from the intersection point between the two linear fitting curves, as reported in **Supplementary Figure S1** 2. The errors associated with these values are calculated with the standard error

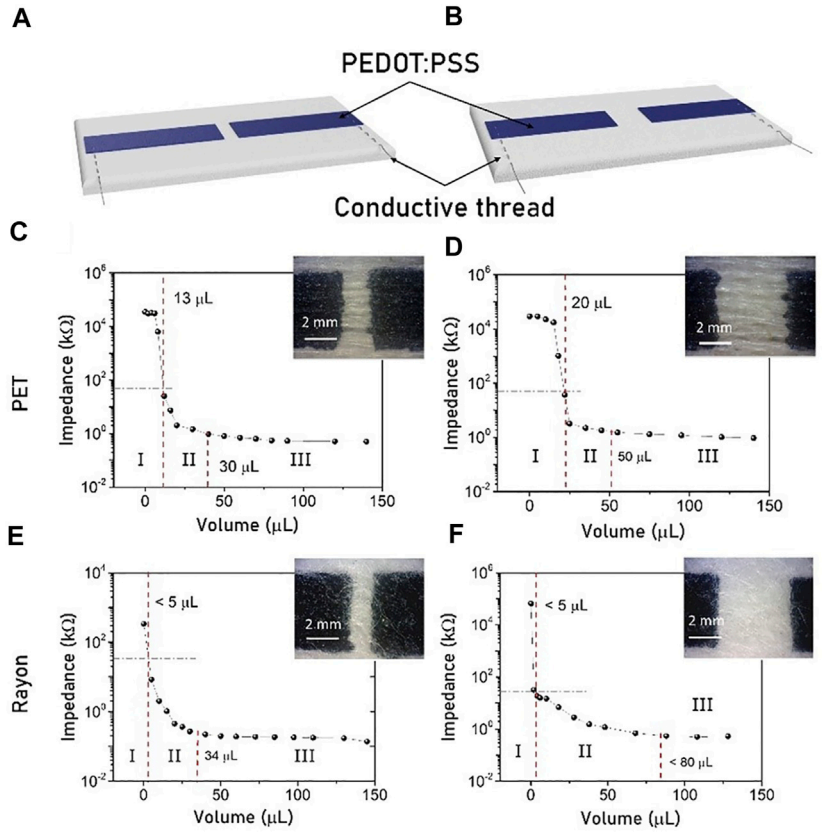


**FIGURE 2 |** Impedance versus exudate volume response for moisture sensors fabricated on the gauze PET **(C–D)** and the gauze Rayon **(E–F)**. Response for different distance between the conductive electrode pads, **(A)** 2 mm and **(B)** 5 mm.

**TABLE 1 |** Moisture sensor parameters in single-layer architecture.

| Gauze | Distance (mm) | V Threshold (µl) | V saturation (µl) |
|---|---|---|---|
| Gauze PET | 2 | 13 ± 3 | 30 ± 2 |
| | 5 | 20 ± 5 | 50 ± 7 |
| Gauze Rayon | 2 | <5 | 34 ± 2 |
| | 5 | <5 | 80 ± 3 |

propagation methods. The recovery feature and the reversibility of the smart moisture sensor were investigated by performing forward/backwards switching cycles from the wet to the dry conditions. The wet state was achieved by pouring 5 µl of simulated exudate onto the sensor, while the dry state was reached speeding up the evaporation process with a hot plate set at 50°C.

# RESULTS

## Single-Layer Sensor

As described in the Material and Methods section, the proposed moisture sensor is based on two electrodes of PEDOT:PSS separated by a defined distance. Before investigating the textile moisture sensor's properties and performance in the final configuration, a simple architecture based on one single layer has been studied. Two different commercial gauzes are compared. The first one, named here "gauze PET", consists of an open mesh fabric based on polyethylene terephthalate (**Figure 1A**) with a thickness of (0.25 ± 0.05) mm. The second one, named "gauze Rayon", consists of a mix of rayon and polyethylene fibres with a thickness of (0.71 ± 0.05) mm (**Figure 1B**). The difference in the composition and weaving structure influences the dispersion of liquid throughout the gauze, as shown in **Figure 1C** and **Figure 1D** for gauze PET and gauze Rayon, respectively. When the same volume of an orange-like color saturated iodine solution is deposited on the centre of (25 × 25) mm pieces of fabric, the liquid broadly spreads over a large area for the gauze PET, while it remains confined in the middle of the gauze Rayon.

These two types of gauzes have been used as active substrate to fabricate a simple moisture sensor configuration based on PEDOT:PSS by screen printing technique. Different volumes of simulated exudate are poured onto the sensor's active part while the impedance is monitored.

**Figure 2** shows the performance of the sensors fabricated onto the gauzes PET and Rayon, changing the distance between the

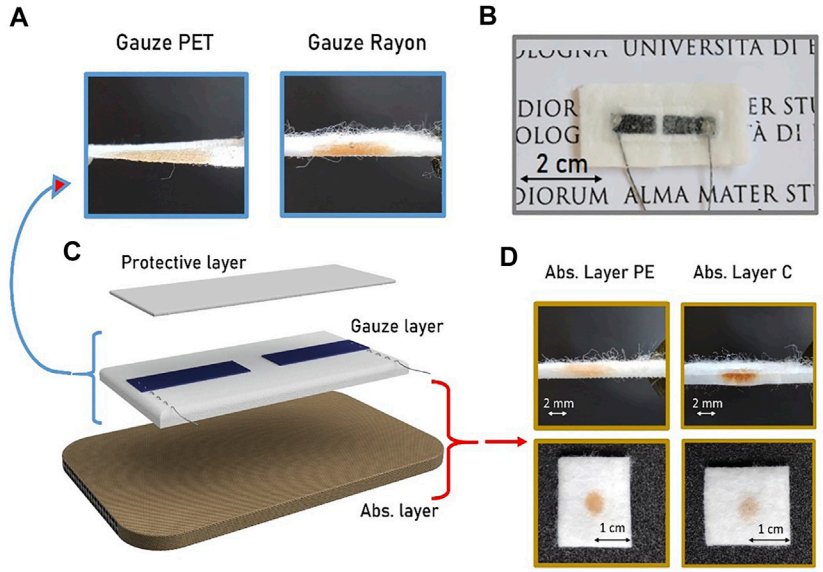


**FIGURE 3 |** Complete moisture sensors architecture. **(A)** Cross section of the Gauzes PET and Rayon with the diffusion profile of a colored drop. **(B)** Optical image of the final textile moisture sensor prototype. **(C)** Structure of the bandage sensor showing the three different composition layers. **(D)** Cross section and top views of the two absorbing layers used as reservoir substrate highlighting their different wettability.

**TABLE 2 |** Physical properties of the layers investigated. The absorption is reported both in g/g and in l/m$^2$ to indicate the amount of volume absorbable by the textile material compared to its initial weight or to its planar dimensions, respectively.

| Layer | Absorption | | Thickness |
|---|---|---|---|
| | g/g | l/m$^2$ | mm |
| Protective Layer | 5.2 ± 0.5 | 0.05 ± 0.01 | 0.12 ± 0.02 |
| Gauze PET | 8.0 ± 1.3 | 0.37 ± 0.03 | 0.20 ± 0.05 |
| Gauze Rayon | 11.0 ± 0.5 | 1.38 ± 0.07 | 0.71 ± 0.05 |
| Abs Layer PE | 10.0 ± 0.7 | 2.2 ± 0.2 | 2.1 ± 0.1 |
| Abs Layer C | 17.1 ± 0.7 | 3.8 ± 0.2 | 2.7 ± 0.1 |

two electrode strips: 2 mm (**Figures 2A,C,E**) and 5 mm (**Figures 2B, D,F**). The response of the single-layer sensor realized on gauze PET is shown in **Figures 2C–D** for the 2 and 5 mm configurations, respectively. Three regimes could be identified in the impedance versus exudate volume plot. In the first dry regime (I), the impedance is high (>10 MOhm), and small additions of exudate (<V threshold) do not affect the sensor response. When the volume of exudate exceeds the threshold volume, the sensor reaches a second regime (II). The ions-rich exudate enables the electrical contact between the electrodes and, exploiting the ionic-electronics conduction properties of PEDOT: PSS, the total impedance starts to decrease.When the amount of exudate is high enough, the impedance reaches a stable value leading the system to reach the saturation regime (third regime, III). Focusing on the final target of a smart bandage for the passive detection of wound moisture, we identify 50 kOhm as the threshold impedance value separating the first dry regime and the second intermediate regime. Similar trends have also been obtained with sensors fabricated on the gauze Rayon, as reported in **Figures 2E–F**. In this specific case, the first dry regime is negligible. Indeed, after the addition of few microliters of simulated exudate (less than 5 µl) the impedance value drops into the second intermediate regime. Threshold and saturation volumes are reported in **Table 1** for both sensors' configurations.

Comparing the results, it is clear that the sensor's performance is strongly affected by gauze properties and composition. The difference in the solution dispersion implies that more exudate is needed to decrease the impedance value of the gauze PET under the identified value of 50 kΩ because it widely spreads over the surface (**Figure 1C**). In the case of the gauze Rayon, the drop stays in the middle of the two electrodes (**Figure 1D**) and leads to a sudden impedance decrease. This is the predominant effect that allows to control and tune the minimum exudate volume needed to activate the required impedance variation (threshold volume), while the distance between the two electrodes exerts a weaker influence on it. On the other hand, the saturation volume is mainly affected by the distance between the electrodes, and with a larger sensing area, more exudate is needed to saturate the sensor's response.

## Bandage Sensor

The previous results underline that different gauze compositions can change the moisture sensor performance. In view of this, a more complex architecture is further investigated, including both tested types of sensing substrates in an actual bandage. The new structure is composed of three different stacked layers. **Figure 3B** shows a top view of the final sensor architecture, while the schematic structure is reported in **Figure 3C**. The first layer is a thin gauze, which is directly in contact with the wound and guarantees biocompatibility and sterility. The second layer is the active gauze containing the moisture sensor. **Figure 3A** shows the cross-section highlighting the different diffusive behavior of

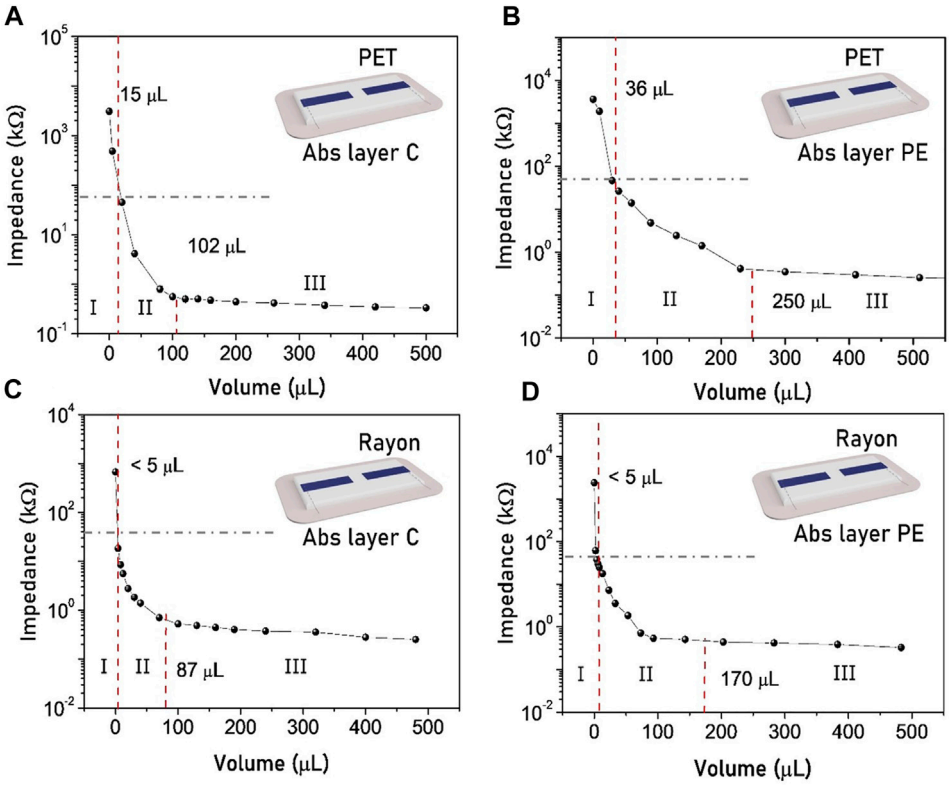


**FIGURE 4 |** Bandage sensor response to the addition of synthetic exudate using the configuration with a 2 mm distance between the electrodes. The dashed lines identify the threshold and the saturation volumes and demarcate the three regimes. The sensors based on gauze PET **(A–B)** show a higher threshold volume than the one based on gauze Rayon **(C–D)**.

**TABLE 3 |** Moisture sensor parameters in different bandage architectures. The spacing between the two electrodes is fixed to 2 mm.

| Gauze | Absorbing layer | V threshold (µL) | V saturation (µL) |
|---|---|---|---|
| GAUZE PET | Abs Layer C | 15 ± 3 | 102 ± 2 |
| | Abs Layer PE | 36 ± 5 | 252 ± 2 |
| GAUZE Rayon | Abs Layer C | 1.7 ± 0.1 | 87 ± 1 |
| | Abs Layer PE | 3.5 ± 0.4 | 170 ± 2 |

liquids through these gauzes. Finally, the bandage is completed with an absorbing layer (**Figure 3D**) that has several tasks: guide the exudate flux through the sensing area, avoid stagnation, collect the total amount of exudate and protect the wound from external impact.

Two different absorbing layers have been investigated and compared. The first one, called Abs Layer PE, is a thick layer of non-woven cotton with an absorption capability of 10 g/g. The second one, called Abs Layer C, is a polyurethane foam attached under a cellulose-based mesh fabric. The thicknesses of the two different substrates are comparable but Abs layer C has an absorption coefficient that almost doubles the other. **Table 2** reports the physical relevant properties of the investigated layers.

The difference in the absorbing layer composition influences the exudate distribution. **Figure 3D** shows the top view and cross-section photographs of the absorbing layers while a drop of colored solutions is dropped onto the surface. Abs Layer PE spreads the liquid in a horizontal direction, while Abs Layer C tends to deliver the liquid downwards, where the C-foam absorbs it by swelling.

Since in the previous paragraph we have established that the influence of the distance between the PEDOT:PSS electrodes has a weak effect on the sensor performance, we tested the final bandage architecture in a configuration with a fixed electrode spacing of 2 mm. The results obtained by the four substrate combinations (gauze Rayon and gauze PET, Abs Layer PE and Abs Layer C) are reported in **Figure 4**.

The behavior of the stacked sensor is slightly different from that of the single-layer sensor. In this case, the first dry regime does not present a plateau and stable impedance values, but decreases right after a small volume addition. Threshold exudate volumes are identified when the impedance reaches the set value of 50 kOhm, and they are reported in **Table 3** together with the saturation volumes. As in the single-layer configuration, the threshold volume is mainly influenced by the gauze type (**Table 1**). On the other side, the saturation volume is affected by the absorbance layer. In particular, even if the Abs Layer PE has a lower absorption capability when it is used in a smart

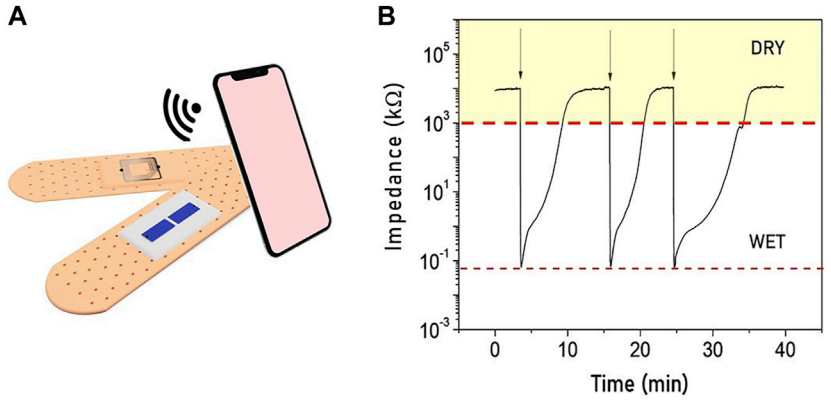


**FIGURE 5 | (A)** Illustration of the smart moisture bandage with the electrodes in the internal parts of the bandage and the RFID tamper alarm on the external side to realize a fully passive device. **(B)** Real-time monitoring of the sensor's impedance when the status switches between wet and dry showing a reversible behavior.

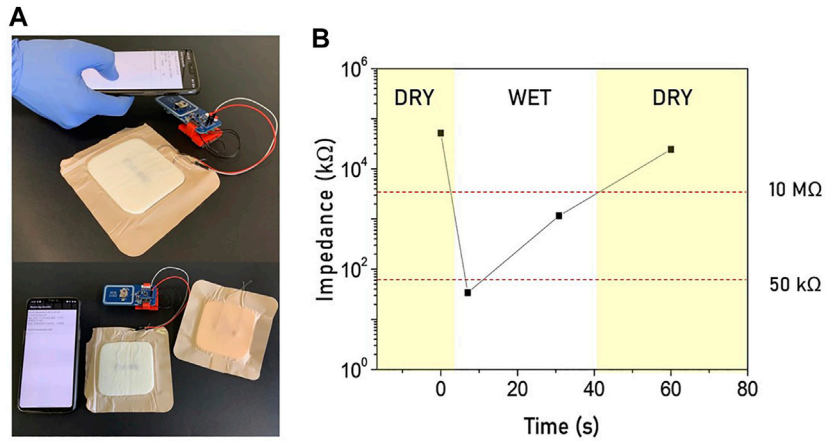


**FIGURE 6 | (A)** Moisture sensor embedded in a real wound dressing and attached to an NFC interface. **(B)** The wireless communication with a NFC reader (a smartphone) allows to perform a quantitative measurement to investigate the wound condition in real-time.

bandage as a reservoir, it leads to a right-shifting in the saturation regime with respect to the bandage fabricated with Abs Layer C. This is mainly related to the different liquid dispersion capability of the absorption layers. Abs Layer C can absorb a higher total volume of exudate, which is accumulated under the sensor, while the Abs Layer PE can spread the liquid among a larger surface area, implying that a higher quantity is needed to saturate the moisture sensor.

## DISCUSSION

After having studied the material's effects on the sensor's performance, the here proposed moisture sensors have been integrated into a "smart" bandage. As assessed in the previous paragraphs, the main feature that affects the sensor response and behavior is the composition of the textile substrate. On the one hand, from the characterization with simulated exudate, the threshold volume at which the impedance drops under the value of 50 kΩ is mainly related to the gauze used as a substrate. On the other hand, the saturation volume depends on the specific properties of the absorption layer. In particular, the absorption coefficient is not the only value that affects the sensor's behavior, but the horizontal distribution of exudate through the textile also has a strong impact. Other parameters, such as the distance between the two printed conductive electrodes, have a lower influence on the sensor performance.

The sensor's large impedance variation recorded when it passes from being dry to wet (**Figure 5B**) allows to directly integrate it with a passive RFID chip, achieving a low cost, passive, humidity sensor tag. The integrated "smart" humidity sensor exploits the RFID's tamper function, similarly to the one proposed by Cramet et al. [31], in which the "tamper bit" changes state (0–1) when impedance varies above and below a threshold.

Upon wireless interrogation, the integrated RFID tag probes the moisture sensor's impedance, and reports back the "tamper

bit" status, with dry status (impedance > thousand kΩ) and wet status (impedance < hundred kΩ). A representation of the final fully passive smart bandage is reported in **Figure 5A**. The sensor impedance has been monitored while the bandage switches from the dry to the wet state several times. As reported in **Figure 5B**, the impedance variation lies in the same range for each cycle, confirming the reliability and the reversibility of the smart moisture sensor.

A proper combination of gauze and absorption layer can thus be used to obtain an entirely passive smart bandage able to give a RFID tamper alarm when the wound switches from wet to dry and vice-versa.

In addition, the moisture sensor has been integrated with a more advanced RFID-NFC tag (NHS3152) to perform quantitative measurements. Upon wireless interrogation, the tag harnesses the RF signal and measures the sensor output connected between two of its terminals (**Figure 6**). The measured value is then read through a smartphone embedded with an NFC reader.

In conclusion, the here presented idea of smart textile moisture sensor allows to combine different commercial textile substrates, which are regularly used for wound care, to design and implement an advanced "smart" wound dressing able to continuously monitor in real time the moisture condition of the wound. Tunable properties and performance can be obtained, depending on the wound type. When a low amount of exudate is present on the wound, the gauze Rayon with the Abs layer C represents a better combination to monitor the wound healing progression. On the opposite, in order to monitor the healing stages of a highly exuding wound, such as chronic wounds or blisters, the gauze PET and Abs layer PE result in a more suitable combination, since it is able to store a large amount of fluid. The possibility to connect the smart textile patch to a RFID and to a NFC interface leads to a fully passive assembled smart bandage for rapid, low-cost, disposable and wireless real-time monitoring of wound moisture.

## DATA AVAILABILITY STATEMENT

The original contributions presented in the study are included in the article/**Supplementary Material**, further inquiries can be directed to the corresponding authors.

## AUTHOR CONTRIBUTIONS

MT; LP substantial contributions to the conception or design of the work, acquisition, analysis and interpretation of data for the work; drafting the work LT; DA substantial contributions to the acquisition of data for the work IG; FM: drafting the work and revising it critically for important intellectual content; ES; BF; FM: revising work critically for important intellectual content; provide approval for publication of the content; MT: agree to be accountable for all aspects of the work in ensuring that questions related to the accuracy or integrity of any part of the work are appropriately investigated and resolved.

## ACKNOWLEDGMENTS

Authors thanks project of Ministero dello Sviluppo Economico–2020–Progetto "Alma Value–Proof of Concept POC per la valorizzazione dei brevetti dell'Alma Mater–Monitoraggio in continuo di pH e idratazione–MIRAGE".

## SUPPLEMENTARY MATERIAL

The Supplementary Material for this article can be found online at: https://www.frontiersin.org/articles/10.3389/fphy.2021.722173/full#supplementary-material

## REFERENCES

1. Tonnesen MG, Feng X, and Clark RAF. Angiogenesis in Wound Healing. *J Invest Dermatol Symp Proc* (2000) 5:40–6. doi:10.1046/j.1087-0024.2000.00014.x
2. Menke NB, Ward KR, Witten TM, Bonchev DG, and Diegelmann RF. Impaired Wound Healing. *Clin Dermatol* (2007) 25:19–25. doi:10.1016/j.clindermatol.2006.12.005
3. Frykberg RG, and Banks J. Challenges in the Treatment of Chronic Wounds. *Adv Wound Care* (2015) 4:560–82. doi:10.1089/wound.2015.0635
4. Dargaville TR, Farrugia BL, Broadbent JA, Pace S, Upton Z, and Voelcker NH. Sensors and Imaging for Wound Healing: A Review. *Biosens Bioelectron* (2013) 41:30–42. doi:10.1016/j.bios.2012.09.029
5. Brown MS, Ashley B, and Koh A. Wearable Technology for Chronic Wound Monitoring: Current Dressings, Advancements, and Future Prospects. *Front Bioeng Biotechnol* (2018) 6:47. doi:10.3389/fbioe.2018.00047
6. Okan D, Woo K, Ayello EA, and Sibbald G. The Role of Moisture Balance in Wound Healing. *Adv Skin Wound Care* (2007) 20:39–53. doi:10.1097/00129334-200701000-00013
7. Lazarus GS, Cooper DM, Knighton DR, Margolis DJ, Percoraro RE, Rodeheaver G, et al. Definitions and Guidelines for Assessment of Wounds and Evaluation of Healing. *Wound Repair Regen* (1994) 2:165–70. doi:10.1046/j.1524-475X.1994.20305.x
8. Dealey C, Cameron J, and Arrowsmith M. A Study Comparing Two Objective Methods of Quantifying the Production of Wound Exudate. *J Wound Care* (2006) 15:149–53. doi:10.12968/jowc.2006.15.4.26897
9. Salvo P, Dini V, Di Francesco F, and Romanelli M. The Role of Biomedical Sensors in Wound Healing. *Wound Med* (2015) 8:15–8. doi:10.1016/j.wndm.2015.03.007
10. Gualandi I, Tessarolo M, Mariani F, Possanzini L, Scavetta E, and Fraboni B. Textile Chemical Sensors Based on Conductive Polymers for the Analysis of Sweat. *Polymers* (2021) 13:894. doi:10.3390/polym13060894
11. Yu L, Yang Z, and An M. Lab on the Eye: A Review of Tear-Based Wearable Devices for Medical Use and Health Management. *Bst* (2019) 13:308–13. doi:10.5582/bst.2019.01178
12. Kim J, Campbell AS, de Ávila BE-F, and Wang J. Wearable Biosensors for Healthcare Monitoring. *Nat Biotechnol* (2019) 37:389–406. doi:10.1038/s41587-019-0045-y
13. Scott C, Cameron S, Cundell J, Mathur A, and Davis J. Adapting Resistive Sensors for Monitoring Moisture in Smart Wound Dressings. *Curr Opin Electrochemistry* (2020) 23:31–5. doi:10.1016/j.coelec.2020.02.017
14. Qin M, Guo H, Dai Z, Yan X, and Ning X. Advances in Flexible and Wearable pH Sensors for Wound Healing Monitoring. *J Semicond* (2019) 40:111607. doi:10.1088/1674-4926/40/11/111607
15. Farooqui MF, and Shamim A. Low Cost Inkjet Printed Smart Bandage for Wireless Monitoring of Chronic Wounds. *Sci Rep* (2016) 6:23955–6900. doi:10.1038/srep28949

16. Mariani F, Serafini M, Gualandi I, Arcangeli D, Decataldo F, Possanzini L, et al. Advanced Wound Dressing for Real-Time pH Monitoring. *ACS Sens.* (2021) 6: 2366–77. doi:10.1021/acssensors.1c00552
17. Kassal P, Kim J, Kumar R, De Araujo WR, Steinberg IM, Steinberg MD, et al. Smart Bandage with Wireless Connectivity for Uric Acid Biosensing as an Indicator of Wound Status. *Electrochemistry Commun* (2015) 56:6–10. doi:10.1016/j.elecom.2015.03.018
18. Galliani M, Diacci C, Berto M, Sensi M, Beni V, Berggren M, et al. Flexible Printed Organic Electrochemical Transistors for the Detection of Uric Acid in Artificial Wound Exudate. *Adv Mater Inter* (2020) 7:2001218. doi:10.1002/admi.202001218
19. Ochoa M, Rahimi R, and Ziaie B. Flexible Sensors for Chronic Wound Management. *IEEE Rev Biomed Eng* (2014) 7:73–86. doi:10.1109/RBME.2013.2295817
20. Mehmood N, Hariz A, Templeton S, and Voelcker N. An Improved Flexible Telemetry System to Autonomously Monitor Sub-bandage Pressure and Wound Moisture. *Sensors* (2014) 14:21770–90. doi:10.3390/s141121770
21. Ma L, Wu R, Patil A, Zhu S, Meng Z, Meng H, et al. Full-Textile Wireless Flexible Humidity Sensor for Human Physiological Monitoring. *Adv Funct Mater* (2019) 29:1904549. doi:10.1002/adfm.201904549
22. Zhou G, Byun J-H, Oh Y, Jung B-M, Cha H-J, Seong D-G, et al. Highly Sensitive Wearable Textile-Based Humidity Sensor Made of High-Strength, Single-Walled Carbon Nanotube/Poly(vinyl Alcohol) Filaments. *ACS Appl Mater Inter* (2017) 9:4788–97. doi:10.1021/acsami.6b12448
23. Devaux E, Aubry C, Campagne C, and Rochery M. PLA/carbon Nanotubes Multifilament Yarns for Relative Humidity Textile Sensor. *J Engineered Fibers Fabrics* (2011) 6:155892501100600–24. doi:10.1177/155892501100600302
24. Li B, Xiao G, Liu F, Qiao Y, Li CM, and Lu Z. A Flexible Humidity Sensor Based on Silk Fabrics for Human Respiration Monitoring. *J Mater Chem C* (2018) 6: 4549–54. doi:10.1039/c8tc00238j
25. Choi KH, Sajid M, Aziz S, and Yang B-S. Wide Range High Speed Relative Humidity Sensor Based on PEDOT:PSS-PVA Composite on an IDT Printed on Piezoelectric Substrate. *Sensors Actuators A: Phys* (2015) 228:40–9. doi:10.1016/J.SNA.2015.03.003
26. Benchirouf A, Palaniyappan S, Ramalingame R, Raghunandan P, Jagemann T, Müller C, et al. Electrical Properties of Multi-Walled Carbon nanotubes/PEDOT:PSS Nanocomposites Thin Films under Temperature and Humidity Effects. *Sensors Actuators B: Chem* (2016) 224:344–50. doi:10.1016/j.snb.2015.10.009
27. Hossein-Babaei F, and Akbari T. Direct Current Powered Humidity Sensor Based on a Polymer Composite with Humidity Sensitive Electronic Conduction. *Appl Phys Lett* (2020) 117:253303. doi:10.1063/5.0030621
28. McColl D, Cartlidge B, and Connolly P. Real-time Monitoring of Moisture Levels in Wound Dressings *In Vitro*: An Experimental Study. *Int J Surg* (2007) 5:316–22. doi:10.1016/j.ijsu.2007.02.008
29. Milne SD, Seoudi I, Al Hamad H, Talal TK, Anoop AA, Allahverdi N, et al. A Wearable Wound Moisture Sensor as an Indicator for Wound Dressing Change: An Observational Study of Wound Moisture and Status. *Int Wound J* (2016) 13:1309–14. doi:10.1111/iwj.12521
30. Possanzini L, Decataldo F, Mariani F, Gualandi I, Tessarolo M, Scavetta E, et al. Textile Sensors Platform for the Selective and Simultaneous Detection of Chloride Ion and pH in Sweat. *Sci Rep* (2020) 10. doi:10.1038/s41598-020-74337-w
31. Cramer T, Fratelli I, Barquinha P, Santa A, Fernandes C, D'Annunzio F, et al. Passive Radiofrequency X-ray Dosimeter Tag Based on Flexible Radiation-Sensitive Oxide Field-Effect Transistor. *Sci Adv* (2018) 4:eaat1825. doi:10.1126/sciadv.aat1825

**Conflict of Interest:** The authors declare that the research was conducted in the absence of any commercial or financial relationships that could be construed as a potential conflict of interest.

**Publisher's Note:** All claims expressed in this article are solely those of the authors and do not necessarily represent those of their affiliated organizations, or those of the publisher, the editors and the reviewers. Any product that may be evaluated in this article, or claim that may be made by its manufacturer, is not guaranteed or endorsed by the publisher.

*Copyright © 2021 Tessarolo, Possanzini, Gualandi, Mariani, Torchia, Arcangeli, Melandri, Scavetta and Fraboni. This is an open-access article distributed under the terms of the Creative Commons Attribution License (CC BY). The use, distribution or reproduction in other forums is permitted, provided the original author(s) and the copyright owner(s) are credited and that the original publication in this journal is cited, in accordance with accepted academic practice. No use, distribution or reproduction is permitted which does not comply with these terms.*